ELSEVIER

European Journal of Pharmacology 342 (1998) 167–175

ejp

Concentration-dependent actions of a new indene derivative, TN-871, in the enteric nervous system

Yoshifumi Katayama *, Kiichiro Morita [1], Keiji Hirai

Department of Autonomic Physiology, Medical Research Institute, Tokyo Medical and Dental University, 2-3-10 Kandasurugadai, Chiyodaku, Tokyo 101, Japan

Received 2 June 1997; revised 13 October 1997; accepted 14 October 1997

Abstract

Intracellular electrical recordings and fluorimetric measurement of intracellular Ca^{2+} concentration ($[Ca^{2+}]_i$) were made from enteric neurons of the guinea-pig myenteric and submucosal plexuses to examine the actions of 2-*n*-butyl-1-(4-methylpiperazinyl)5,6-ethylendioxyindene · 2HCl (TN-871) on neural activity in the single cell. TN-871 affected neuronal electrophysiological properties and synaptic transmission in the enteric nervous system in a concentration-dependent manner; TN-871 at lower concentrations hyperpolarized enteric neurons and/or facilitated synaptic transmission, whereas at higher concentrations it depolarized enteric neurons and/or inhibited synaptic transmission. Experiments with fura-2 showed that TN-871 modulated both resting $[Ca^{2+}]_i$ and $[Ca^{2+}]_i$-transient associated with action potentials. Thus, the present results demonstrated that TN-871 at lower concentrations facilitates but at higher concentrations depresses Ca^{2+}-dependent or Ca^{2+}-involving processes, suggesting that TN-871 may affect the Ca^{2+} dynamics in enteric neurons either directly, indirectly or both. © 1998 Elsevier Science B.V.

Keywords: Enteric neurons; Indene derivative; Ca^{2+} concentration, intracellular; Synaptic transmission; Transmitter release

1. Introduction

Considerable efforts have been made to develop medicines designed for maintaining or improving brain activities. An indene derivative, indeloxazine, is reported both to possess activating effects on cerebral functions, enhancing the acquisition of learned behavior and desynchronizing the spontaneous EEG activity in rats (Yamamoto and Shimizu, 1987), and to augment long-term potentiation in guinea-pig hippocampal slices (Sugimura et al., 1989). A new indene derivative, 2-*n*-butyl-1-(4-methylpiperazinyl)-5,6-methylenedioxyindene · 2HCl (TN-871) is suggested to have anti-anoxic effects in mice (Ikeda et al., 1991). Our recent study disclosed concentration-dependent dual actions of TN-871 on transmitter release. This was found by using the quantal analysis method applied to nicotinic, fast excitatory postsynaptic potentials (EPSPs) recorded from bullfrog sympathetic ganglion cells; TN-871 at 30 nM facilitated transmitter release but at 3 μM depressed it (Shen et al., 1995).

The enteric nervous system is known to be similar in histology to the central nervous system and to include enteric reflex circuits composed of various types of neurons and complex synaptic transmission systems (Furness and Costa, 1987). Since neither the actions of TN-871 on neuronal activity nor those on synaptic transmission in the enteric nervous system have been documented, the present electrophysiological experiments were undertaken. Also, from time to time, intracellular Ca^{2+} concentration ($[Ca^{2+}]_i$) was simultaneously monitored by using a fluorescent Ca^{2+} indicator, fura-2, because Ca^{2+} is widely known to be involved in controlling neuronal activity and synaptic transmission. This paper describes concentration-dependent opposite cellular actions of TN-871 in the enteric nervous system and possible involvement of Ca^{2+} in the TN-871 actions.

* Corresponding author. Tel.: +81-3-52808078; fax: +81-3-52808077.
[1] Present Address: Department of Psychiatry, Kurume University School of Medicine, 67 Asahimachi, Kurume 830, Japan.

2. Materials and methods

Adult guinea-pigs were lightly anesthetized with ether and then stunned and bled from the neck. Myenteric and submucosal plexuses were isolated from the ileum and caecum, respectively, mounted in a small chamber (volume, 0.5 ml) and visualized with a differential interference contrast microscope at total magnification of 200 or 500 ×. The preparations were continuously superfused with a modified Krebs solution of the following composition (mM): NaCl 117, KCl 4.7, $CaCl_2$ 2.5, $MgCl_2$ 1.2, NaH_2PO_4 1.2, $NaHCO_3$ 25 and glucose 11.5. The superfusing solution was saturated with 95% O_2 and 5% CO_2 and maintained at about 35–36°C. TN-871 was applied by superfusion at various concentrations.

Intracellular recordings were made with microelectrodes having tip resistances of 40–60 MΩ and filled with 1–2 M KCl. Small hyperpolarizing current pulses (strength: 0.1–0.3 nA, duration: 50–100 ms and frequency: 0.1–1 Hz) were applied to detect changes in the cellular input resistance during experiments (see Figs. 2, 5 and 6). Intracellular signals were monitored, digitized, and stored by means of a memory oscilloscope (VC-10, Nihon-Kohden), and directly or subsequently displayed on a chart recorder (RECTI-HORIZ, San-ei). Individual neurons were identified as S and AH neurons according to their electrophysiological characteristics (Nishi and North, 1973; Hirst et al., 1974; Bornstein et al., 1994). Synaptic potentials, fast and slow excitatory postsynaptic potentials (EPSPs) and inhibitory postsynaptic potentials (IPSPs), were evoked by focal stimulation to ganglia or strands of nerve fibers connecting ganglia, using glass-capillary electrodes, having a tip diameter of 5–10 μm and containing Krebs solution. Nicotinic acetylcholine potentials were caused by ionophoresis (40–100 nA for 40–100 ms) using micropipettes filled with acetylcholine (0.5 M) in the presence of atropine if necessary; and a retaining current (5–10 nA) was continuously passed to prevent leakage of acetylcholine from the pipettes. Similarly, noradrenaline hyperpolarizations were produced by ionophoresis (40–100 nA for 1–2 s) from micropipettes filled with noradrenaline (0.1 M) with a backing current (5–10 nA).

The $[Ca^{2+}]_i$ of individual neurons was optically monitored using a fluorescent Ca^{2+} indicator, fura-2, as reported previously (Tatsumi et al., 1988; Hirai et al., 1996). Fura-2 was ionophoretically injected into somata of enteric neurons through recording microelectrodes which contained 0.5 mM fura-2 in 1 M KCl solution. An inverted microscope (TMD, Nikon) was modified for the present purpose and equipped with a dichroic mirror (DM-455). Fura-2 was excited by the light from a Xenon lamp passed through interference filters (340, 360 and 380 nm with 10 nm half-bandwidth, Ditric Optics). Emission from neurons loaded with fura-2 was filtered using a barrier cut-off filter at 500 nm, and the intensity of the fluorescence was measured with a photomultiplier tube (R 1635, Hamamatsu Photonics), having been recorded on a pen recorder chart through a current–voltage converter. The intensity when excited by 380 nm was denoted by F380, and when excited by 340 nm by F340, and so on. $[Ca^{2+}]_i$ was estimated from the intensity of the fura-2 fluorescence using either the two-wavelength method or the single wavelength method (Grynkiewicz et al., 1985). In the case of the single wavelength method, F380 was mainly measured, and F340 and F360 were recorded before, after or during each recording and from time to time in order to calculate $[Ca^{2+}]_i$ and/or to verify experimental conditions such as intracellular fura-2 concentrations.

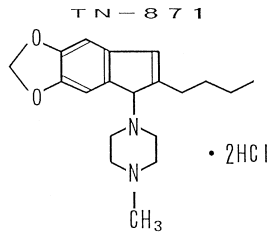

Fig. 1. The structural and molecular formula of TN-871 (2-*n*-butyl-1-(4-methylpiperazinyl)-5,6-methylenedioxyindene·2HCl).

Drugs used were TN-871 (Fig. 1, gift from Taiyo Pharmaceutical), acetylcholine chloride, atropine sulfate monohydrate, L-noradrenaline bitartrate (Wako Pure Chemical Industries) and fura-2 (Dojindo). The results are expressed as means ± S.E.M. of the number of observations in parentheses. Statistical significance was evaluated using Students paired *t*-test.

3. Results

According to their electrophysiological characteristics, enteric neurons are classified into two types, S and AH neurons (see Section 2). The present results were obtained from both S and AH neurons which had resting membrane potentials higher than −50 mV and action potentials higher than 60 mV in amplitude. Steady intracellular recordings longer than 30 min were obtainable in the present experiments.

3.1. Actions of TN-871 on enteric neurons

3.1.1. Resting membrane potential and neuronal input resistance

TN-871 (30 nM–10 μM) caused membrane depolarizations and/or hyperpolarizations in both S and AH neurons. These actions were concentration-dependent, as shown in Fig. 2; here, effects of TN-871 were examined on 28 S

neurons (18 myenteric and 10 submucosal) and 13 AH neurons (10 myenteric and 3 submucosal).

3.1.1.1. S neurons. TN-871 at 10 and 30 nM did not affect the resting membrane potential and input resistance ($n = 4$, for each). TN-871 at concentrations higher than 100 nM for myenteric and 300 nM for submucosal neurons caused a membrane depolarization associated with an increase in input resistance (Fig. 2A-a). This increase was also clear when the depolarization was manually eliminated by passing a hyperpolarizing current (manual voltage-clamp method: DC in Fig. 2A-a). The amplitude of TN-871-induced depolarizations was dependent on the drug concentration, as shown in Fig. 2A-b.

3.1.1.2. AH neurons. As shown in Fig. 2B-a, TN-871 at 100 nM caused a membrane hyperpolarization and at 1 μM induced a transient hyperpolarization followed by depolarization. TN-871 at concentrations higher than 3 μM caused only depolarizations in AH neurons without the preceding transient hyperpolarization. It is speculated that the transient hyperpolarization might be due to the transient exposure of the preparations to a lower concentration of TN-871. Concentration–response relationships in AH neurons are shown in Fig. 2B-b, where the transient hyperpolarization was not included. The hyperpolarization was associated with a decrease in membrane input resistance, whereas the depolarization was accompanied by an increase in the input resistance (Fig. 2B-a). These changes in membrane resistance were also evident when the depolarization and hyperpolarization caused by TN-871 were manually eliminated by passing direct current (DC in Fig. 2B-a).

3.1.1.3. Reversal potential of the depolarizing and hyperpolarizing responses induced by TN-871. The reversal potentials of the TN-871-induced responses were estimated from the current–voltage relationships which were obtained before, during and after the TN-871-induced responses. The reversal potentials for the depolarization at 1 μM in S and AH neurons were -83 ± 3.0 mV ($n = 4$) and -87 ± 3.1 mV ($n = 4$), respectively. The reversal potential for the hyperpolarization at 100 nM in AH neurons was -87 ± 2.0 mV ($n = 4$). These values are

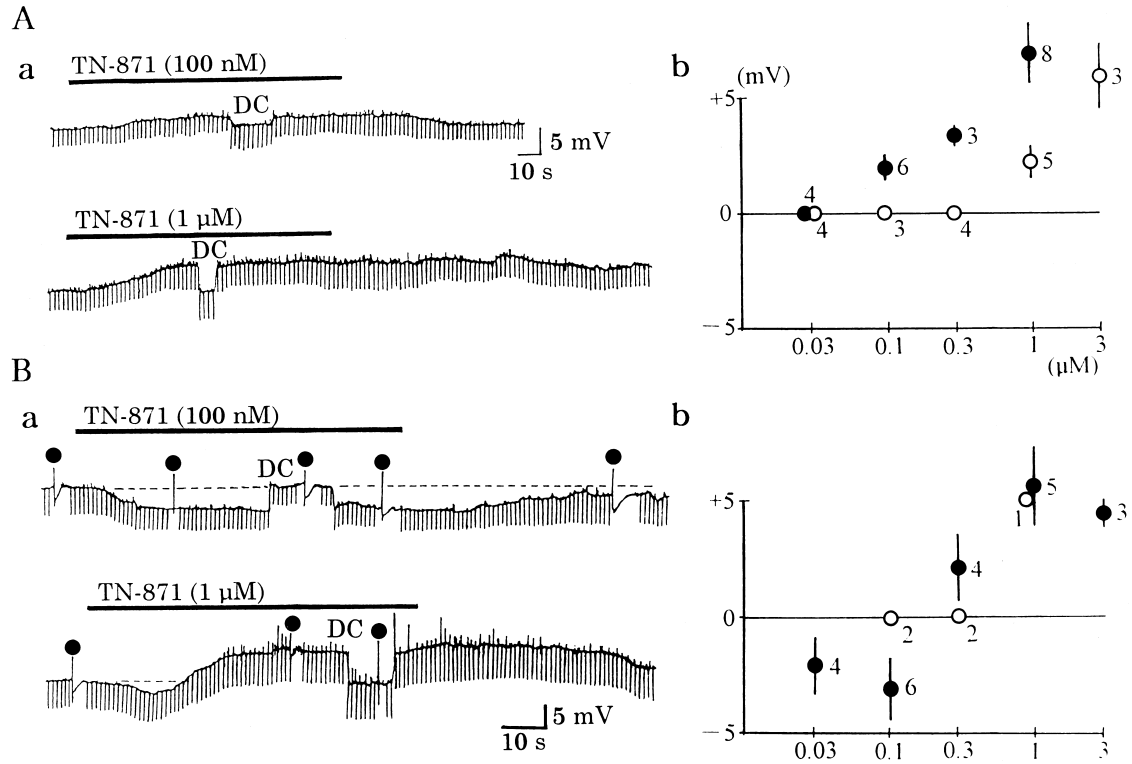

Fig. 2. Effects of TN-871 on membrane potential of enteric S (A) and AH (B) neurons. (A-a) and (B-a), intracellular recordings were made from myenteric S (A-a) and AH neurons (B-a). TN-871 at the concentrations indicated was applied by superfusion during the period indicated by horizontal bars. Hyperpolarizing electrotonic potentials were induced by current pulses of 0.2 nA, and direct currents (DC) were passed to eliminate the potential changes induced by TN-871 (manual voltage-clamp method). In (B-a), action potentials were evoked by depolarizing current pulses (indicated by filled circles). (A-b) (S neurons) and (B-b) (AH neurons), the peak amplitude of membrane depolarization and hyperpolarization was plotted on the ordinate against the concentration of TN-871 on the abscissa with the number of observations indicated by attached numerals; filled and open circles indicate the mean value for myenteric and submucosal neurons, respectively, and vertical bars indicate S.E.M. An initial transient hyperpolarization as shown in the bottom trace of (B-a) was not included in the graphs.

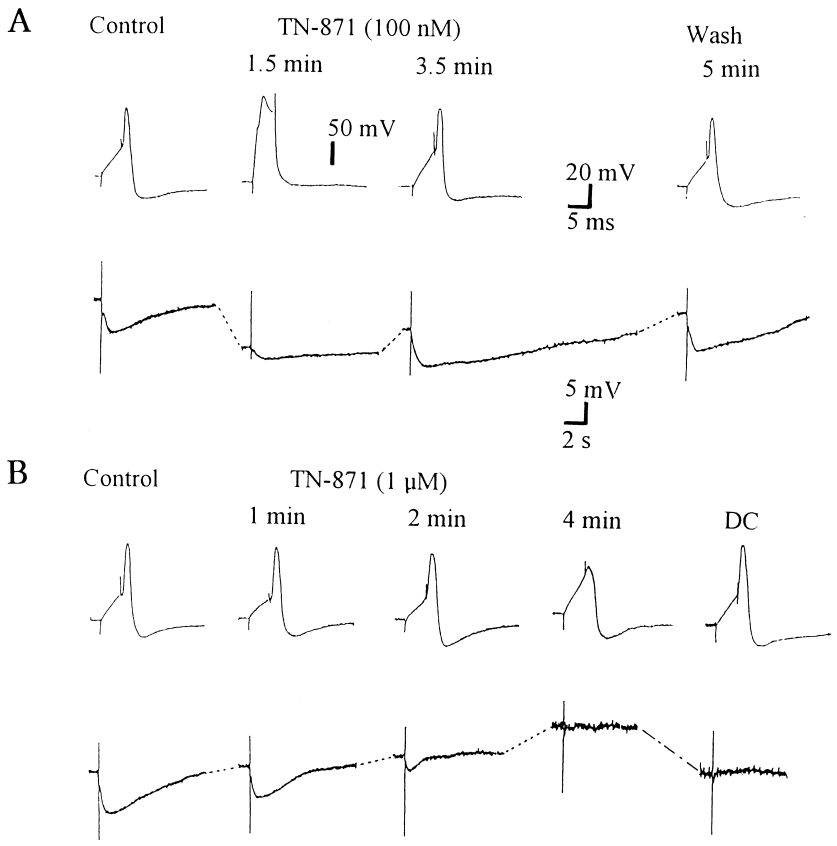

Fig. 3. Effects of TN-871 on action potentials and following after-hyperpolarizations of myenteric AH neurons. Action potentials were evoked by depolarizing current pulses (duration, 5 ms). Lower traces show action potentials, followed by fast phase of the after-hyperpolarizations and long-lasting phase of after-hyperpolarizations (slow after-hyperpolarizations). The initial portion of each lower trace is shown in the corresponding upper trace with fast time scale. (A) TN-871 at 100 nM caused membrane hyperpolarization (dotted line) and this hyperpolarization began to pass off during the presence of TN-871; compare 1.5 min and 3.5 min. (B) TN-871 at 1 μM induced membrane depolarization (dotted line), and the depolarization was manually eliminated by passing an inward direct current (interrupted line and DC). Note that the amplitude of the fast phase of after-hyperpolarization (rightmost, DC) was almost the same as that of the control (leftmost).

most likely to be close to the K^+ equilibrium potential, suggesting that the depolarization and hyperpolarization induced by TN-871 might be due to inactivation and activation of K^+ conductances, respectively.

3.1.2. Action potential and subsequent after-hyperpolarization

The amplitude and width of action potentials were affected by TN-871 (Fig. 3). However, when TN-871-induced changes in membrane potential were manually eliminated as shown on the rightmost (DC) part of Fig. 3B, action potentials in control and DC were almost the same shape. Therefore, it was considered that an apparent change in their shape might be secondarily/indirectly brought about by the TN-871-induced depolarization, because a similar alteration could be observed when the membrane was artificially depolarized by passing outward currents through the recording electrode. It should be added that, when the membrane potential was kept at the control level by the manual voltage-clamp method, the after-hyperpolarization of S neurons (data not shown) and fast phase of the

Table 1
Effects of TN-871 on fast EPSPs

	Myenteric plexus	Submucosal plexus
	fast EPSPs	fast EPSPs
30 nM	154 ± 16^a ($n = 4$) AP+ ($n = 2$)	114 ± 3^a ($n = 3$)
100 nM	106 ± 14 ($n = 8$) AP+ ($n = 5$) and AP− ($n = 2$)	115 ± 13 ($n = 3$)
300 nM	78 ± 12 ($n = 3$)	92 ± 5 ($n = 3$) AP− ($n = 2$)
1 μM	57 ± 14^a ($n = 5$)	50 ± 6^b ($n = 3$) AP− ($n = 3$)
3 μM	66, 0 ($n = 2$)	44 ± 18^a ($n = 3$) AP− ($n = 2$)

% Amplitude of the fast EPSPs in the presence of TN-871 compared to control (100%). Mean ± S.E.M. with the number of observations in parenthesis. When fast EPSPs evoked action potentials, the amplitude of the EPSPs could not be measured. Then, AP−: fast EPSP triggering an action potential in the control failed to trigger it in the presence of TN-871, and AP+: fast EPSP evoking no action potential in the control evoked it in the presence of TN-871.
[a] $P < 0.05$ and [b] $P < 0.01$, compared to control (before TN-871 application).

after-hyperpolarization of AH neurons (see Fig. 3B) were not substantially affected by TN-871 at the concentrations tested.

The slow after-hyperpolarization characteristic of AH neurons was strongly depressed during the TN-871 hyperpolarization (Fig. 2B-a and Fig. 3A), but was almost the same as the control when the hyperpolarization was eliminated (see DC in Fig. 2B-a). However, TN-871 application longer than 3.5 min augmented and markedly prolonged the slow after-hyperpolarization after the membrane hyperpolarization had started disappearing (Fig. 3A). Furthermore, the slow after-hyperpolarization was still augmented even 5 min after washout of TN-871. On the other hand, while the membrane was depolarized with TN-871 at concentrations higher than 1 μM, the slow after-hyperpolarization was inhibited or almost abolished (see Fig. 2B-a and Fig. 3B for myenteric and Fig. 6B for submucosal AH neurons). This inhibition of the slow after hyper-polarization was still observed even when the depolarization was eliminated by passing a hyperpolarizing current (DC in Fig. 2B-a and Fig. 3B).

3.2. Actions of TN-871 on synaptic transmission

3.2.1. Fast EPSPs

The effects of TN-871 on fast EPSPs at various concentrations are summarized in Table 1. TN-871 at 30 nM augmented, but at 100 nM and 1 μM it inhibited fast

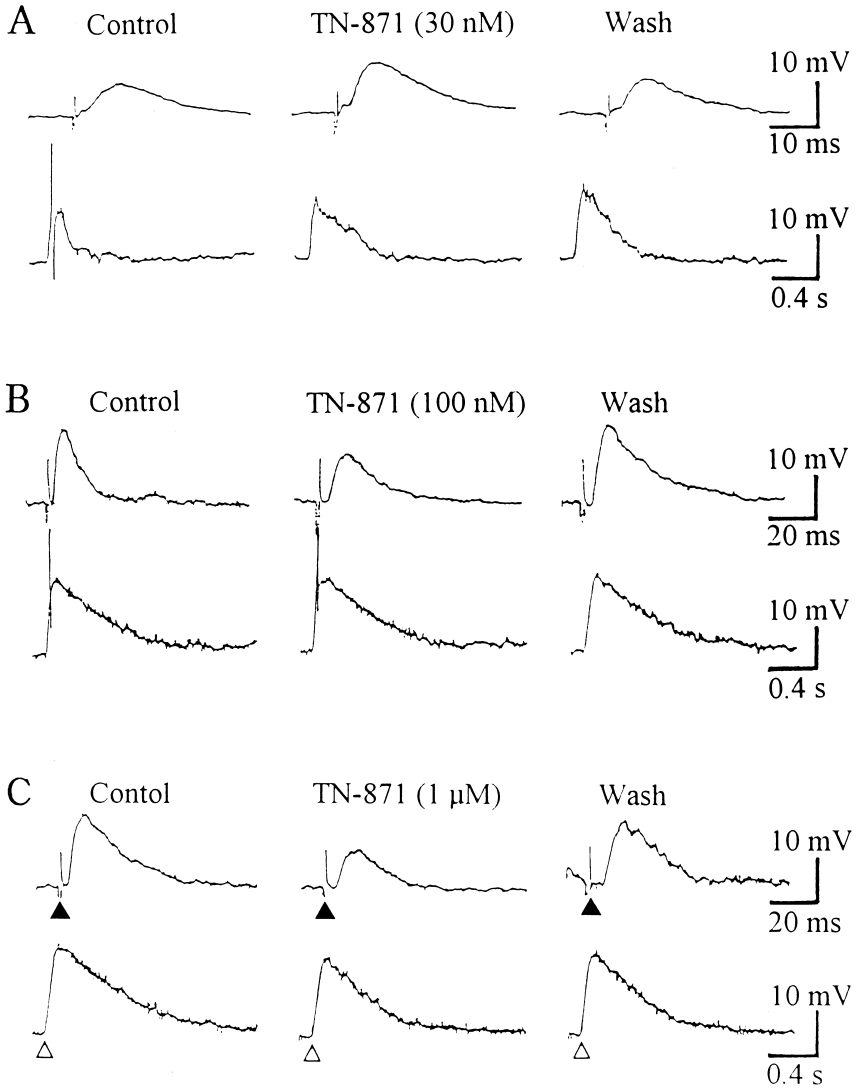

Fig. 4. Effects of TN-871 on fast EPSPs (upper trace) and acetylcholine potentials (lower trace). Fast EPSPs evoked by single electrical focal stimulation (filled arrow head) and acetylcholine potential by its ionophoresis (100 nA for 40 ms, open arrow head) were recorded in pairs from myenteric S neurons. The effects of TN-871 were examined at three concentrations; (A) 30 nM; (B) 100 nM; and (C) 1 μM. Since TN-871 at 100 nM and 1 μM caused a membrane depolarization (3 and 5 mV, respectively), these depolarizations were manually eliminated during recordings of fast EPSPs and acetylcholine potentials. Records in (B) and (C) were obtained from the same neuron. Note the time scale for fast EPSPs in (A) is different from that in (B) and (C).

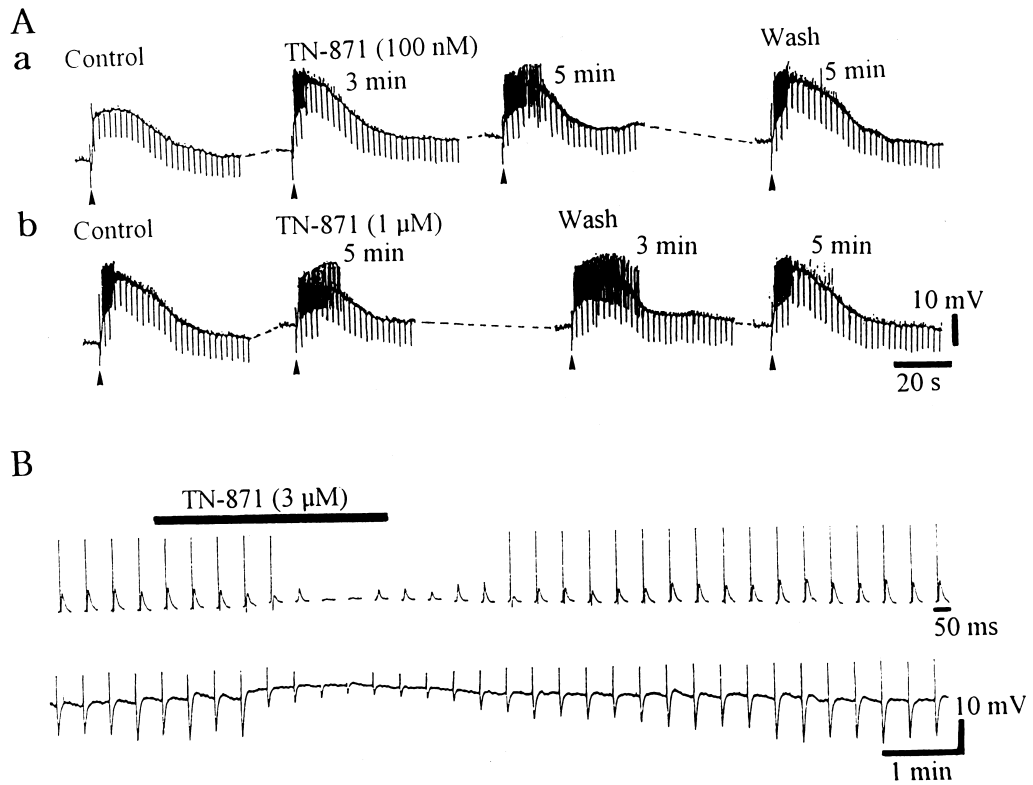

Fig. 5. Effects of TN-871 on slow EPSPs and IPSPs. (A) Slow EPSPs induced by repetitive focal stimulation (10 Hz for 1 s) were recorded from a myenteric S neuron every 3 min. TN-871 (a, 100 nM and b, 1 μM) caused membrane depolarization (dotted line). Hyperpolarizing electrotonic potentials were evoked by current pulses (0.2 nA). (B) Fast EPSPs and IPSPs evoked by single focal stimulation every 20 s were recorded from a submucosal S neuron. Each fast EPSP is shown in upper trace with fast chart speed. TN-871 at 3 μM caused membrane depolarization. In (A) and (B), action potentials were not fully recorded with a pen-recorder.

EPSPs without or with a change in membrane potential (Fig. 4). All records in Fig. 4 were made while the TN-871-induced depolarizations were eliminated manually.

Since the neurotransmitter mediating the fast EPSP is known to be acetylcholine, it was examined whether or not TN-871 might modulate the postsynaptic sensitivity to exogenous acetylcholine. The amplitude of the acetylcholine potentials was hardly affected by TN-871 at 30 nM, 100 nM and 1 μM compared to the fast EPSPs (Fig. 4), indicating that TN-871 might not change the postsynaptic sensitivity to acetylcholine. Therefore, it is concluded that TN-871 might modulate the fast EPSP presynaptically by changing the amount of acetylcholine released from presynaptic nerves. However, TN-871 at very high concentrations (10-30 μM) sometimes affected acetylcholine potentials by decreasing their amplitude (data not shown).

As shown in Fig. 5B, single electrical stimulation evoked a fast EPSP which triggered an action potential in the control but not in the presence of TN-871 at high concentrations, indicating depression of the fast EPSP (AP- in Table 1). On the contrary, the fast EPSP which failed to trigger an action potential in the control became able to trigger an action potential when superfused with low concentrations of TN-871, indicating facilitation of the fast EPSP (AP + in Table 1).

3.2.2. Slow EPSPs and IPSPs

Slow EPSPs were evoked by repetitive focal stimulation (10 Hz for 1 s every 1–3 min). As shown in Fig. 5A, TN-871 at 1 μM decreased the amplitude of slow EPSPs to $54 \pm 10\%$ of the control ($n = 3$, $P < 0.05$). However, the drug at 100 nM changed the amplitude only to $113 \pm 12\%$ of the control ($n = 3$, not significant).

IPSPs caused by single focal stimulation in submucosal S neurons were inhibited by TN-871 at 3 μM as shown in Fig. 5B. TN-871 at 1 and 3 μM decreased the amplitude of IPSPs to $53 \pm 18\%$ ($n = 6$, $P < 0.05$) and to $21 \pm 11\%$ ($n = 4$, $P < 0.05$) of the respective controls, whereas the drug at 30 and 100 nM changed the amplitude only to $101 \pm 7\%$ ($n = 3$, not significant) and $102 \pm 11\%$ ($n = 4$, not significant) of controls. Furthermore, TN-871 at 1 μM did not affect the amplitude of hyperpolarizing responses induced by exogenous noradrenaline. Therefore, since noradrenaline is known to be the neurotransmitter for the slow IPSP, it is assumed that TN-871 at 1 μM could decrease the amount of noradrenaline released from presynaptic terminals without affecting the postsynaptic sensitivity to noradrenaline.

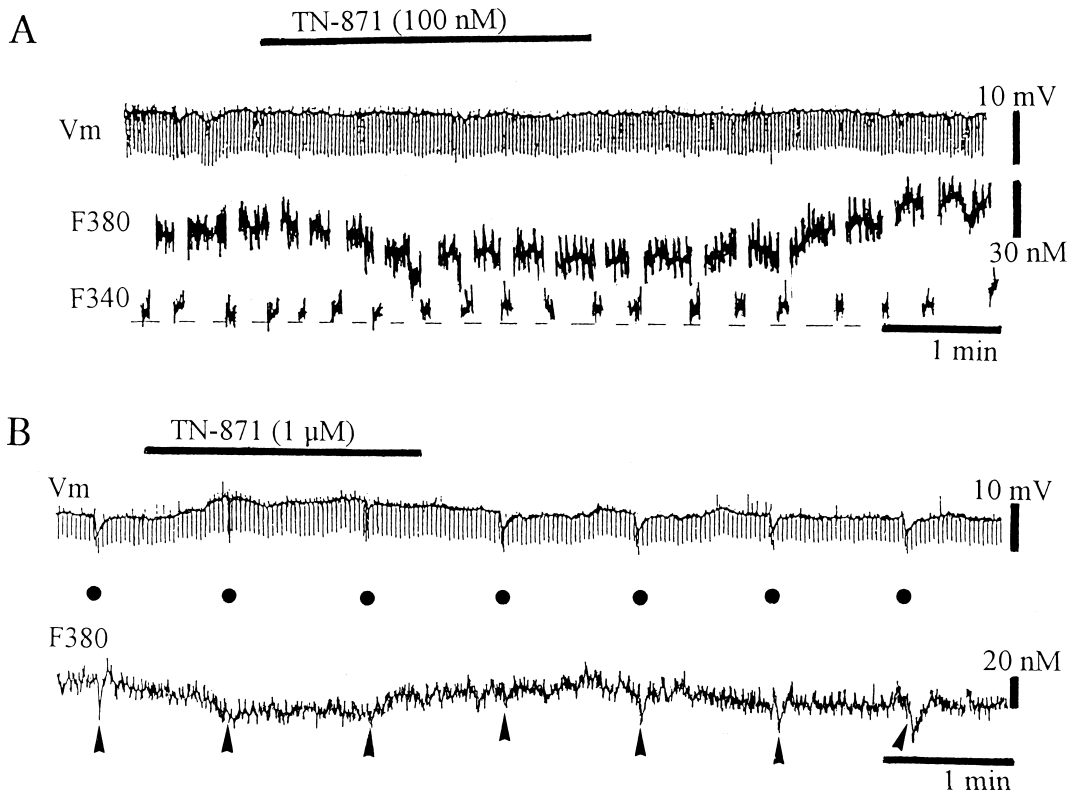

Fig. 6. Effects of TN-871 on electrical properties and $[Ca^{2+}]_i$. TN-871 at the concentrations indicated was applied by superfusion during the period indicated by horizontal bars. Intracellular voltage recordings (mV) and fluorescence intensity recordings ((A) F380 and F340; and (B) F380) were made at the same time. A downward deflection of F380 and an upward one of F340, both indicate an increase in $[Ca^{2+}]_i$. Hyperpolarizing electrotonic potentials were evoked by current pulses (0.2 nA). (A) TN-871 at 100 nM increased $[Ca^{2+}]_i$ without affecting membrane properties in a submucosal S neuron. $[Ca^{2+}]_i$ was estimated at 187 nM before and 228 nM during TN-871 application. (B) TN-871 at 1 μM increased $[Ca^{2+}]_i$ and caused a membrane depolarization in a submucosal AH neuron. $[Ca^{2+}]_i$ was estimated at 130 nM before and 145 nM during TN-871 application. A train of five depolarizing pulses passed through the recording microelectrode (10 Hz) evoked action potentials (filled circle, not fully recorded on a pen-recorder) followed by a slow after-hyperpolarization and a transient $[Ca^{2+}]_i$-increase (arrow head).

3.3. Effects of TN-871 on $[Ca^{2+}]_i$

Simultaneous recordings of membrane potential and $[Ca^{2+}]_i$ were made from 14 submucosal neurons. TN-871 at 100 nM increased $[Ca^{2+}]_i$ to 121 ± 2.0% of the control ($n = 3$, $P < 0.01$); Fig. 6A shows that $[Ca^{2+}]_i$ was elevated to 122% of the control (from 187 to 228 nM) without a change in membrane potential. The increase in $[Ca^{2+}]_i$ with 100 nM of the drug was abolished in Ca^{2+}-free/6 mM Mg^{2+} solution, in which the resting $[Ca^{2+}]_i$ was lowered.

Fig. 6B shows that TN-871 at 1 μM increased $[Ca^{2+}]_i$ to 114% of the control (from 127 to 145 nM) and also depolarized the membrane. However, this increase was almost reversed when the TN-871-induced depolarization was eliminated ($n = 3$, see Section 4). Furthermore, a small decrease in $[Ca^{2+}]_i$, by about 5% of the control, was observed from two neurons showing no membrane depolarization at 1 μM. Summarizing, the TN-871-induced change in $[Ca^{2+}]_i$ to 107 ± 4.9% of control ($n = 7$) was not significant at 1 μM.

It should be noted that, in Fig. 6B, the slow after-hyperpolarization (filled circle) and the $[Ca^{2+}]_i$-transient (arrowhead) associated with each action potential were almost abolished at 1 μM of TN-871. But the $[Ca^{2+}]_i$-transient in two submucosal AH neurons was not affected at 100 nM (see below, Section 4).

4. Discussion

It was demonstrated that TN-871 showed concentration-dependent, opposite effects on membrane properties and synaptic transmission in the guinea-pig enteric nervous system. That is, TN-871 at lower concentrations hyperpolarized enteric neurons (only myenteric AH neurons) and facilitated synaptic transmission, but at higher concentrations it depolarized the enteric neurons and inhibited synaptic transmission. These electrophysiological results are consistent with those obtained with optical measurement of $[Ca^{2+}]_i$, as discussed below.

The slow after-hyperpolarization of AH neurons is generated by opening of Ca^{2+}-sensitive K^+ channels regulated

by Ca^{2+} that entered during action potentials through voltage-dependent Ca^{2+} channels (Morita et al., 1982; Hirst et al., 1985). Since TN-871 at high concentrations depressed the $[Ca^{2+}]_i$-transient associated with the action potential, the inhibition of the slow after-hyperpolarization might be due partly to blockade of voltage-dependent Ca^{2+} entry, though the types of Ca^{2+} channels involved remain to be identified. On the other hand, no detectable change in the $[Ca^{2+}]_i$-transient was observed at a lower concentration; indeed, TN-871 at 100 nM did not affect the slow after-hyperpolarization when the membrane potential was fixed at the resting level.

In the present experiments, TN-871 at 100 nM induced a membrane hyperpolarization and/or an increase in the resting $[Ca^{2+}]_i$, neither of which was observed in Ca^{2+}-free/high Mg^{2+} solution. The hyperpolarization was associated with a decrease in input resistance and was reversed in polarity near the K^+ equilibrium potential. It is suggested that the hyperpolarization was possibly the result of activation of Ca^{2+}-sensitive K^+ channels by increasing Ca^{2+} influx. On the other hand, TN-871 at 1 μM caused a membrane depolarization, reversed in polarity near the K^+ equilibrium potential, and apparently elevated $[Ca^{2+}]_i$. This $[Ca^{2+}]_i$-increase was, however, abolished or even converted to a decrease when the depolarization was manually eliminated (see Tatsumi et al., 1988). Then, it is likely that the depolarization was partly brought about by inactivation of Ca^{2+}-sensitive K^+ channels in myenteric AH neurons (Grafe et al., 1980; North and Tokimasa, 1987; Katayama and Morita, 1992). All of these findings suggested that TN-871 could affect the resting Ca^{2+} influx in a concentration-dependent manner, resulting in changes in the resting $[Ca^{2+}]_i$ which regulates Ca^{2+}-sensitive K^+ channels.

The present results showed that TN-871 modulated the fast EPSPs and IPSPs without changing the acetylcholine and noradrenaline potentials, indicating that TN-871 might modulate neurotransmitter release from presynaptic nerve terminals without altering postsynaptic sensitivity to acetylcholine and noradrenaline. Our previous study with quantal analysis identified the presynaptic site of actions of TN-871 on acetylcholine release in the bullfrog sympathetic ganglion (Shen et al., 1995). Release of neurotransmitter is believed to be coupled to transient elevation of $[Ca^{2+}]_i$ at release sites (Zucker and Lando, 1986), and voltage-dependent Ca^{2+} entry during presynaptic action potentials is known to be an important step for transmitter release (Stanley and Atrakchi, 1990). Then, although TN-871 is supposed to affect Ca^{2+} channels in the release sites, it is technically difficult to observe their behavior in presynaptic terminals of the present preparations. Observations from the soma may provide some clues as to the mechanism underlying the presynaptic actions of TN-871, as follows. The $[Ca^{2+}]_i$-transient was inhibited at 1 μM, possibly by depressing voltage-dependent Ca^{2+} entry, but was not affected at 100 nM. The resting $[Ca^{2+}]_i$ was elevated at 100 nM possibly because of an increase in resting Ca^{2+} influx. Thus, it is likely that $[Ca^{2+}]_i$ of presynaptic terminals might be elevated at low concentration of TN-871. Furthermore, it is also assumed that TN-871 might directly or indirectly affect a cytosolic Ca^{2+} buffering system by controlling the rate of Ca^{2+} sequestration and by changing the amount of intracellular Ca^{2+} buffering proteins. In this context, it should be noted that the slow after-hyperpolarization was markedly prolonged during long-lasting application and even after washout of TN-871 (100 nM, Fig. 3A).

It is pointed out that Ca^{2+} plays a critical role in a variety of pathological and toxicological processes (see Orrenius et al., 1989). A Ca^{2+} set-point with an optimal concentration of intracellular Ca^{2+} is hypothesized for neuronal survival (Collins et al., 1991; Koike and Tanaka, 1991). In this regard it is likely that TN-871 at a low concentration might facilitate or maintain neuronal activity and at high concentrations might prevent the neuronal death which is considered to be due to excess accumulation of internal Ca^{2+}. Neuronal activity might be enhanced via activation of synaptic transmission. Indeed, TN-871 at 30 nM augmented synaptic transmission, possibly by acting as a Ca^{2+} ionophore and increasing the resting Ca^{2+} entry in release sites, as in myenteric AH neurons, in which low concentrations of TN-871 caused membrane hyperpolarization due to an increase in Ca^{2+}-sensitive K^+ conductance but not in S neurons (see above). On the other hand, a possible action of TN-871 at higher concentrations as a Ca^{2+} channel blocker might be involved in preventing internal Ca^{2+} accumulation leading to neuronal death. In fact, TN-871 at higher concentrations inhibited synaptic transmission mainly as a result of depression of voltage-dependent Ca^{2+} influx in presynaptic terminals. A decrease in the amount of the released excitatory neurotransmitter might also contribute to prevention of internal Ca^{2+} accumulation mediated by receptors. All of these findings suggest that TN-871 might activate neuronal functions at lower concentrations and might prevent neuronal injury or death at higher concentrations.

Acknowledgements

This work was supported in part by a Grant-in-Aid for Scientific Research from the Ministry of Education, Science and Culture of Japan. The authors wish to thank Taiyo Pharmaceutical Industry Co. Ltd., Tokyo for the supply of TN-871.

References

Bornstein, J.C., Furness, J.B., Kunze, W.A.A., 1994. Electrophysiological characterization of myenteric neurons: How do classification schemes relate?. J. Auton. Nerv. Syst. 48, 1–15.

Collins, F., Schmidt, M.R., Guthrie, P.B., Kater, S.B., 1991. Sustained increase in intracellular calcium promotes neuronal survival. J. Neurosci. 11, 2582–2597.

Furness, J.B., Costa, M., 1987. The Enteric Nervous System. Churchill Livingstone, Edinburgh.

Grafe, P., Mayer, C.J., Wood, J.D., 1980. Synaptic modulation of calcium-dependent potassium conductance in myenteric neurones in the guinea-pig. J. Physiol. (London) 305, 235–248.

Grynkiewicz, G., Poenie, M., Tsien, R.Y., 1985. A new generation of Ca^{2+} indicators with greatly improved fluorescence properties. J. Biol. Chem. 260, 3440–3450.

Hirai, K., Katayama, Y., Misu, Y., 1996. L-DOPA induces concentration-dependent facilitation and inhibition of presynaptic acetylcholine release in the guinea pig submucous plexus. Brain Res. 718, 105–111.

Hirst, G.D.S., Holman, M.E., Spence, I., 1974. Two types of neurones in the myenteric plexus of the duodenum in the guinea pig. J. Physiol. (London) 236, 303–326.

Hirst, G.D.S., Johnson, S.M., Helden, D.F., 1985. The slow calcium-dependent potassium conductance in a myenteric neurone of the guinea-pig ileum. J. Physiol. (London) 361, 315–337.

Ikeda, N., Hara, S., Fujii, A., Yokochi, E., 1991. Anti-anoxic effect of TN-871 in mice. Jpn. J. Pharmacol. 55, 208.

Katayama, Y., Morita, K., 1992. Substance P inhibit activation of calcium-dependent potassium conductances in guinea-pig myenteric neurones. J. Physiol. (London) 447, 293–308.

Koike, T., Tanaka, S., 1991. Evidence that nerve growth factor dependence of sympathetic neurons for survival in vitro may be determined by levels of cytoplasmic free Ca^{2+}. Proc. Natl. Acad. Sci. USA 88, 3892–3896.

Morita, K., North, R.A., Tokimasa, T., 1982. The calcium-activated potassium conductance in guinea-pig myenteric neurones. J. Physiol. (London) 329, 341–345.

Nishi, S., North, R.A., 1973. Intracellular recording from the myenteric plexus of the guinea-pig ileum. J. Physiol. (London) 231, 471–491.

North, R.A., Tokimasa, T., 1987. Persistent calcium-sensitive potassium current and the resting properties of guinea-pig myenteric neurones. J. Physiol. (London) 386, 333–353.

Orrenius, S., McConkey, D.J., Bellomo, G., Nicotera, P., 1989. Role of Ca^{2+} in toxic cell killing. Trends Pharmacol. Sci. 10, 281–285.

Shen, Y.L., Hirai, K., Katayama, Y., 1995. Effects of an indene-derivative, TN-871, on synaptic transmission in a sympathetic ganglion: Presynaptic actions on neurotransmitter release. Bull. Tokyo Med. Dent. Univ. 42, 19–29.

Stanley, E.F., Atrakchi, A.H., 1990. Calcium currents recorded from a vertebrate presynaptic nerve terminal are resistant to the dihydropyridine nifedipine. Proc. Natl. Acad. Sci. USA 87, 9683–9687.

Sugimura, M., Ishihara, K., Katsuki, H., Satoh, M., 1989. Indeloxazine augments long-term potentiation in the mossy fiber-CA3 system of guinea-pig hippocampal slices. J. Pharmacobio-Dyn. 12, 771–774.

Tatsumi, H., Hirai, K., Katayama, Y., 1988. Measurement of the intracellular calcium concentration neurons by using fura-2. Brain Res. 451, 371–375.

Yamamoto, M., Shimizu, M., 1987. Cerebral activating properties of indeloxazine hydrochloride. Neuropharmacology 26, 761–770.

Zucker, R.S., Lando, L., 1986. Mechanism of transmitter release: Voltage hypothesis and calcium hypothesis. Science 231, 574–579.